DØnote 5127-Conf

Version: 5.0
Primary Author(s): Olav Mundal

Comments to d0-run2eb-014@fnal.gov
by June 1st

Search for the Associated Production of Chargino and Neutralino in Final States with Two Electrons and an Additional Lepton

The DØ Collaboration
URL: http://www-d0.fnal.gov
(Dated: June 7, 2006)

A search has been performed for the trilepton decay signature from the associated production of the lightest chargino and the next-to-lightest neutralino in leptonic channels with two electrons within the context of minimal Supersymmetry. The search uses data taken with the DØ detector at the Fermilab Tevatron $p\bar{p}$ collider at a center-of-mass energy of 1.96 TeV corresponding to an integrated luminosity of 1.1 fb^{-1}. No candidates have been found, with an expected background of 0.76 ± 0.67 events. In combination with results in three other trilepton search channels, new stringent limits on the associated production of charginos and neutralinos have been set.

Preliminary Results for Summer 2006 Conferences

I. INTRODUCTION

Supersymmetry (SUSY [1]) postulates a symmetry between bosonic and fermionic degrees of freedom and predicts the existence of a supersymmetric partner for each standard model particle. The present analysis searches for the associated production of the charged and neutral partners of the electroweak gauge and Higgs bosons (charginos and neutralinos) in final states with two electrons, a third lepton and large missing transverse energy. The analysis is based on the Minimal Supersymmetric extension of the Standard Model (MSSM) with R-parity conservation [1]. The model predicts the associated production of the lightest chargino ($\tilde{\chi}_1^\pm$) and the next-to-lightest neutralino ($\tilde{\chi}_2^0$) at $\mathrm{p\bar{p}}$ colliders with subsequent decays into fermions and the LSP (the lightest supersymmetric particle, $\tilde{\chi}_1^0$) [2]. This note describes the search for purely leptonic decay modes using a selection of final states with two electrons and a third track, optimized for the process $\mathrm{p\bar{p}} \rightarrow \tilde{\chi}_1^\pm \tilde{\chi}_2^0 \rightarrow \ell ee \nu \tilde{\chi}_1^0 \tilde{\chi}_1^0$. As a guideline, the results are interpreted using a model motivated by the more specific minimal supergravity with chargino and neutralino masses mainly following the relation $m_{\tilde{\chi}_1^\pm} \approx m_{\tilde{\chi}_2^0} \approx 2m_{\tilde{\chi}_1^0}$. The points in mSUGRA parameter space considered here are characterized by slepton masses close to the chargino/neutralino masses, which lead to an enhanced leptonic branching fraction. The chargino/neutralino decay mode depends on the mass relation to the scalar partners of the charged leptons (sleptons). The present note focuses on 3-body decays via off-shell gauge bosons and sleptons (see Fig. 1), which are enhanced with respect to the cascade decay via sleptons for slepton masses comparable or larger than the chargino/neutralino masses. For simplicity, the result is interpreted in a scenario without slepton mixing and degenerate $\tilde{\mathrm{e}}_\mathrm{R}$, $\tilde{\mu}_R$ and $\tilde{\tau}_\mathrm{R}$ masses. Searches for supersymmetric particles have been performed in $\mathrm{e}^+\mathrm{e}^-$ collisions at LEP [3] and in $\mathrm{p\bar{p}}$ collisions at DØ [4], [5] and CDF [6]. No evidence for these particles has been found so far. LSP masses below 40 GeV are excluded in MSSM models with GUT relations by the LEP experiments. In mSUGRA, the LSP lower mass limit is found at 50-60 GeV [3]. For large slepton/sneutrino masses, chargino masses are excluded nearly up to the kinematic production threshold of 103 GeV at LEP [3] by direct searches. Higgs searches at LEP yield indirect sensivity also for the mass region beyond the chargino production threshold.

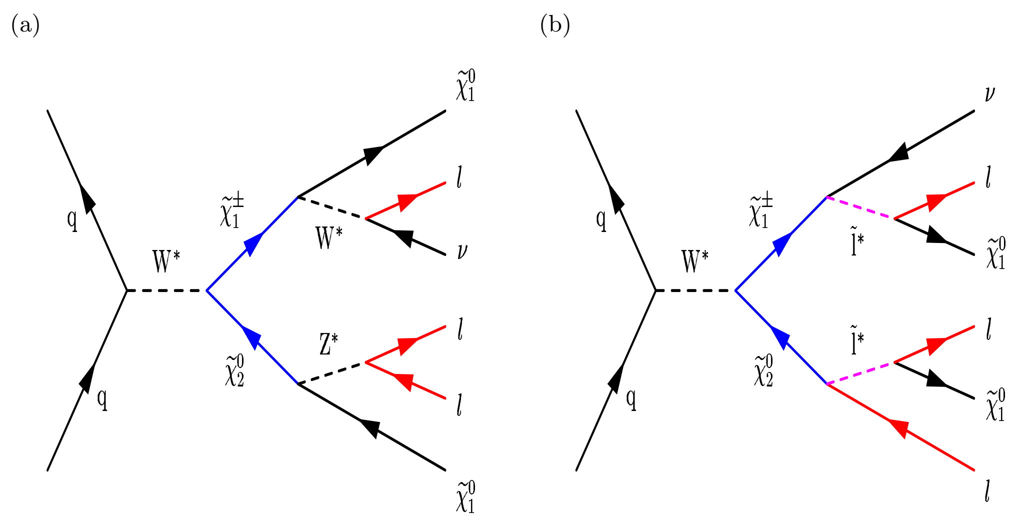

FIG. 1: Main production and decay modes for the signal points considered in the present analysis.

II. DATA AND MC SAMPLES

The analysis is based on data collected from April 2002 to February 2006 by the DØ detector at the Fermilab Tevatron $\mathrm{p\bar{p}}$ collider at a center-of-mass energy of 1.96 TeV and corresponds to an integrated luminosity of 1.1 fb^{-1}. The luminosity is determined by normalizing MC to data around the Z peak at preselection level, using the NNLO cross section 241.6 pb. All simulated signal and standard model processes are generated using PYTHIA 6.319 [7] and processed through the full detector simulation. Signal parameter combinations have been generated for $\tan\beta = 3$ and chargino masses in the range of 98-150 GeV using the Les Houches Accords, (LHA) [9]. See table I. Three reference points were chosen with low, medium and high $\tilde{\chi}^\pm$ mass within this mass range. The symbols in table I are: The common fermion mass at GUT scale, $m_{1/2}$, the common scalar mass at GUT scale, m_0, the ratio of vacuum expectation values of the two Higgs fields, tanβ, the trilinear coupling A_0 and the Higgs(ino) mass parameter, μ. The total cross section $\sigma \times$ BF($p\bar{p} \rightarrow \tilde{\chi}_1^{\pm}\tilde{\chi}_2^0 \rightarrow 3\ell$) varies between 0.5 and 0.1 pb. A detailed description of the generated reference points is given in Table I. Major background sources are $Z/\gamma \rightarrow ee$, $W + \gamma \rightarrow e\nu + \gamma$, and $WW \rightarrow ee\nu\nu$. Multijet background from QCD production is determined directly from data. For this, a sample dominated by multijet background has been defined that are identical to the search sample except a reversed lepton identification requirements. The resulting sample corresponds to dijet events that are broader than the jets which are actually preselected in the analysis. To correct this sample for trigger dependencies, the subsample of the data with like-sign electrons is used. The like sign sample is dominated by QCD events at preselection level, but cannot be used in advanced stages of the analysis, since the signal is partly like sign. All standard selection cuts are applied to the QCD sample with reversed lepton identification requirements, except cuts that strongly correlate with the reversed cut. For these cuts, the rejection is estimated from the like sign sample. The QCD sample is normalized at an early stage of the selection in the low mass region.

name	$\tilde{\chi}^{\pm}$-mass (GeV)	$\tilde{\chi}_2^0$-mass (GeV)	$\tilde{\chi}_1^0$ mass (GeV)	m_0 (GeV)	$m_{1/2}$ (GeV)	$m_{\tilde{l}_R}$ (GeV)	$\sigma \times BR[pb]$
LHA.244.324	150	152	82	121	221	153	0.058
LHA.131.232	125	127	69	98	192	129	0.14
LHA. 87.194	115	118	63	88	182	119	0.22

TABLE I: Susy parameters for three reference signal points. All points have tan$\beta = 3$, $A_0 = 0$, $\mu > 0$.

III. EVENT SELECTION

The selection procedure is summarized briefly in Table II. It will be justified and described in more detail in the following.

The selection requires two electrons with $p_T > 8, 12$ GeV with high electromagnetic energy fraction and passing energy isolation cuts. They are required to match in η and ϕ with a reconstructed track. An electron likelihood, [10], based on tracking and calorimeter quantities is used to further enhance the purity of the electron sample. Both electrons must stem from the primary vertex and be reconstructed in detector pseudorapidity $|\eta| < 3.0$ with at least one electron in the central region (detector $|\eta| < 1.1$). To reduce the background from photon conversions, at least one hit in the silicon tracking detector (SMT) is required for the next-to-leading electron. This requirement is replaced by a tightened likelihood cut for events with a vertex outside the SMT acceptance.

Figure 2a shows the distribution in data, background and signal of the invariant dielectron mass at this stage of the selection. This stage is referred to as preselection stage. Most of the $Z/\gamma^* \rightarrow ee$ events are rejected by requiring the invariant dielectron mass to be in the range $18\,\text{GeV} < M < 60\,\text{GeV}$. A large fraction of remaining back-to-back $Z/\gamma^* \rightarrow ee$ is reduced by requiring the opening angle between the leptons to be less than 2.9. The $t\bar{t}$ contribution is reduced by requiring H_T to be lower than 80 GeV. H_T is defined as the scalar sum of the transverse momenta of all jets in the event.

TABLE II: Summary of the event selection

(1) Preselection	$p_T > 8\,\text{GeV}, 12\,\text{GeV}$ electrons large electron likelihood electrons from primary vertex at least one electron in the central calorimeter at least 1 Hit in the inner SMT for $\mid z0 \mid < 35$cm likelihood tightened for $\mid z0 \mid > 35$cm
(2) Anti $Z/\gamma^* \rightarrow ee$	$18\,\text{GeV} < \text{inv. mass} < 60\,\text{GeV}$ $\Delta\phi(e, e) < 2.9$
(3) Anti-Top	anti $t\bar{t}$: $H_T < 80\,\text{GeV}$
(4) Isolated Track	$p_T^{\ell 3} > 4.0\,\text{GeV}$ isolation $\Sigma p_T < 1$ GeV, $E_{iso} < 3$ GeV
(5) $\not{E}_T$ related	$\not{E}_T > 22\,\text{GeV}$ transverse mass (e+$\not{E}_T$) $> 20\,\text{GeV}$ Sig ($\not{E}_T$) > 8.0
(6) Tr$\times\not{E}_T$	$\not{E}_T \times p_T^{\ell 3} > 220\text{GeV}^2$

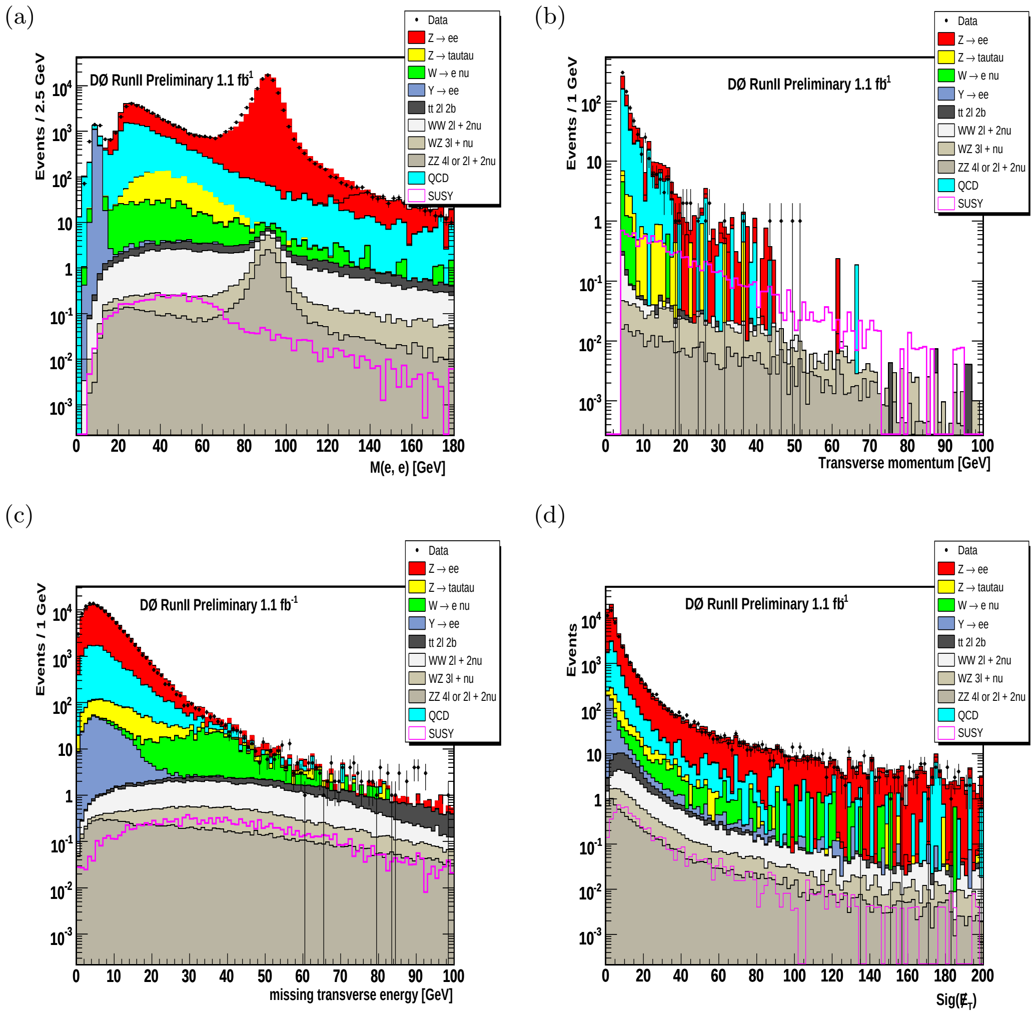

FIG. 2: Distribution of (a) the invariant dielectron mass at preselection level (b) the isolated track transverse momentum, $p_T^{\ell 3}$, just before the requirement of an isolated track in the event is made (c) the missing transverse energy, $\not\!\!E_{\rm T}$, at preselection level and (d) the scaled missing transverse energy, Sig($\not\!\!E_{\rm T}$), at preselction level for data (points with error bars), background simulation (histograms, complemented with the QCD expectation) and signal expectation for point LHA.131.232 (empty histogram).

The background at this stage consists mostly of $Z/\gamma^* \to$ ee, $W \to e\nu$, and QCD events, and is significantly reduced by requiring an additional isolated track, well-separated from the two electron candidates ($\Delta R = \sqrt{(\Delta\eta)^2 + (\Delta\phi)^2} > 0.4$) and also stemming from the primary vertex. To ensure a good p_T measurement, either at least 17 hits in the tracking systems where at least one is in the fiber tracker or 14 hits in the fiber tracker are required. Tracks in jets are typically very close to other low-p_T particles, as opposed to the signal where the third track is expected to be isolated. Isolation is ensured by requiring the activity in a hollow cone $0.1 < \Delta R < 0.4$ around the track to be small. The cone is chosen to be hollow to also be efficient from tracks from τ decays, since all tau decay modes (leptonic, hadronic (1 prong), hadronic (3 prong)) either produce only 1 track or a set of tracks in a very narrow cone. Track isolation is done in two steps. First the p_T sum of other reconstructed tracks in the hollow cone is required to be less than 1 GeV. Then the calorimeter energy deposition in a $0.2 < \Delta R < 0.4$ is required to be less than 3 GeV and $\frac{\Sigma E_T}{GeV} < 60\% \sqrt{\frac{p_T^{\ell 3}}{GeV}}$ where $p_T^{\ell 3}$ denotes the p_T of the isolated track. Figure 2b shows the $p_T^{\ell 3}$ distribution just before the requirement of an isolated track in the event is made.

Since the LSP and the neutrinos typically cause a considerable amount of missing energy in the event, a cut on $\not\!\!E_{\rm T}$ will further reduce dijet and $Z/\gamma^* \to$ ee background. Figure 2c shows the distribution in data background and signal of the $\not\!\!E_{\rm T}$ at preselection stage. Events with $\not\!\!E_{\rm T} < 22\,{\rm GeV}$ are discarded. In addition, events are rejected if they contain jets with transverse energies above 15 GeV and have a small significance, Sig($\not\!\!E_{\rm T}$), which is defined by normalizing the $\not\!\!E_{\rm T}$ to $\sigma(E_T^j \| \not\!\!E_{\rm T})$, a measure of the jet energy resolution projected onto the $\not\!\!E_{\rm T}$ direction:

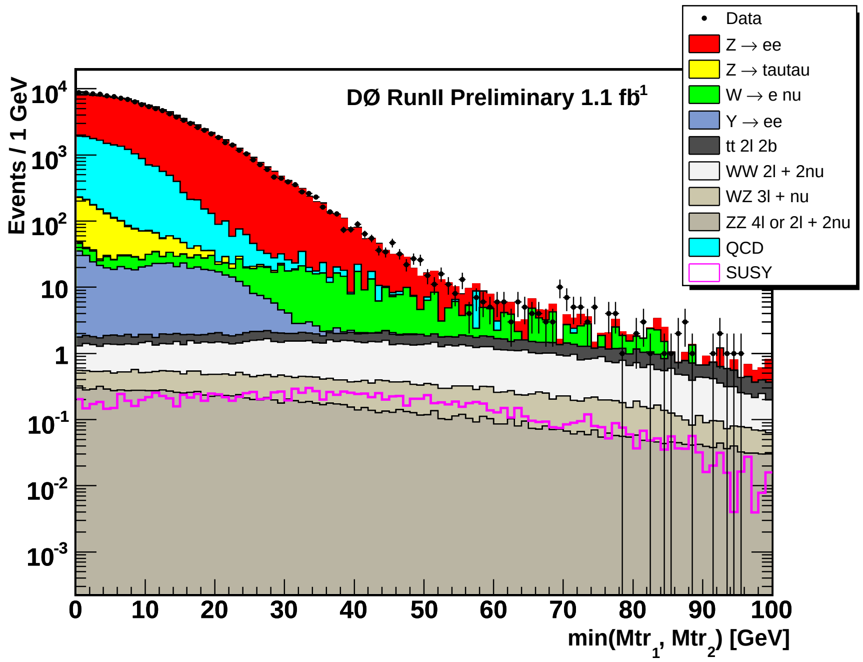

FIG. 3: Distribution of the minimum transverse mass at preselection level in data (points with error bars), background simulation (histograms, complemented with the QCD expectation) and signal expectation for SUSY point LHA.131.232.

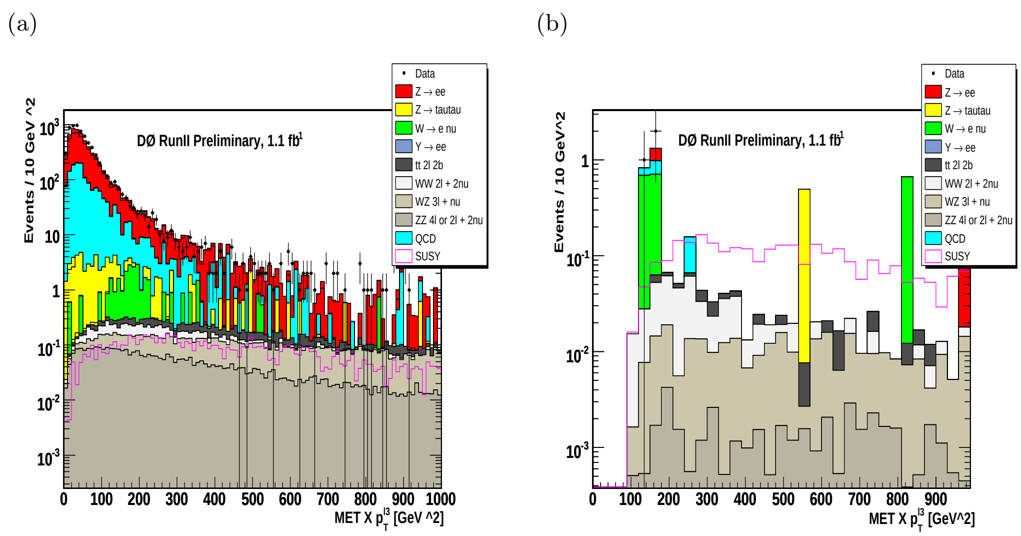

FIG. 4: Distribution of the product of $\not{E}_T$ and $p_T^{\ell 3}$ (a) at preselection level in events with isolated track and (b) after $\not{E}_T$ related cuts, for data (points with error bars), background simulation (histograms, complemented with the QCD expectation) and signal expectation for point LHA.131.232 (empty histogram).

$$\mathrm{Sig}(\not{E}_T) = \frac{\not{E}_T}{\sqrt{\sum_{\mathrm{jets}} \sigma^2_{E_T^j \| \not{E}_T}}}.$$

Figure 2d shows the distribution in data, background and signal of the scaled $\not{E}_T$ at preselection level. Events with a Sig($\not{E}_T$), lower than 8 are discarded.

TABLE III: Number of candidate events observed and background events expected at different stages of the selection. Errors are statistical.

Cut	Data	Sum BG	$Z/\gamma \rightarrow$ee	W$\rightarrow$eν	Z$\rightarrow \tau\tau$	WW/WZ	WZ	fakes
(1) Presel	118518	113713±175	95885±119	499±17	1029±18	83±0.43	18±0.4	16037±95
(2) Anti-Z	17459	16993±89	11053±51	297±12	287±11	26±0.33	2.01±0.04	6698 ±66
(3) Isolated Track	776	624±18	281±8	7.86±2.07	12±2	0.80±0.02	0.79±0.03	347±13
(4) $\not\!\!E_{\rm T}$ related	2	2.02±0.73	0.16±0.16	1.77±0.73	0.32±0.32	0.43±0.02	0.46±0.02	0.48±0.28
(5) Tr$\times\not\!\!E_{\rm T}$	0	0.76±0.67	0.0±0.16	0.0 ±0.59	0.32±0.32	0.14±0.011	0.25±0.01	0.00±0.09

In order to reduce background with large $\not\!\!E_{\rm T}$ due to a poorly measured electron energy, events with an electron-$\not\!\!E_{\rm T}$ transverse mass below 20 GeV are discarded. Figure 3 shows the minimum transverse mass distribution at preselection level.

At this stage, a large fraction of the remaining background consists of W production, where both the second electron and the third track originate from jets. To suppress this particular background component, a tightened cut on the p_T on the third track is applied if the transverse mass between the leading electron and $\not\!\!E_{\rm T}$ is compatible with the W mass. If $M_T > 65$ GeV, the p_T of the isolated track is required to be greater than 7 GeV. To further reduce $Z/\gamma^* \rightarrow$ ee event where one electron is lost, the invariant mass between the isolated track and the leading electron was calculated. In such events, the lost electron is reconstructed as the third track and the second electron is a fake. If the invariant mass was between 60 GeV and 120 GeV and the track is out of the acceptance of electromagnetic calorimeter, the event is discarded. Remaining $Z/\gamma^* \rightarrow$ ee events and QCD are expected to have both low values of $\not\!\!E_{\rm T}$ and $p_T^{\ell 3}$. Figure 4 shows the distribution in $\not\!\!E_{\rm T} \times {\rm p}_{\rm T}^{\ell 3}$ for data, background and signal at preselection level in events with an isolated track (left) and after $\not\!\!E_{\rm T}$related cuts to the right. The product of $\not\!\!E_{\rm T}$ and ${\rm p}_{\rm T}^{\ell 3}$ is required to be larger than 220 $(\,{\rm GeV})^2$.

IV. SYSTEMATIC UNCERTAINTIES

The estimates for expected numbers of background and signal events depend on numerous measurements that each introduce a systematic uncertainty: trigger efficiencies (1–2%), lepton identification and reconstruction efficiencies (1–2%), jet energy scale calibration in signal ($< 4\%$) and background events (7–20%), lepton and track momentum calibration (2%), detector modeling (1% for signal, 5–10% for background), PDF uncertainties ($< 4\%$), and modeling of multijet background (4%). The systematic error on the luminosity is mainly a combination of the PDF uncertainty (4%) and (3.5%) uncertainty for the NNLO Zee cross section. In total, the systematic uncertainty on signal is 5.2% and 25% on background. However, the systematic error is small compared to the statistical error for the background.

V. RESULTS

Numbers of observed candidates and background events expected after application of the successive selections are listed in table III. The selected data and background events are in agreement and no candidate is selected. The background expectation is $0.76 \pm 0.67 \pm 0.19$ events, dominated by $Z/\gamma^* \rightarrow \tau\tau$ and di-boson events. The number of signal events is in the range of 1.7-4.7 events in the final selection for the three reference points mentioned in this note. Table IV shows the number of signal events expected at different stages of the cutflow for the three signal points discussed in the $ee\ell$ analysis. Since no evidence for associated production of charginos and neutralinos is observed, an upper limit on the product of cross section and leptonic branching fraction $\sigma \times {\rm BR}(3\ell)$ is extracted from this result. The result of this analysis is combined with the results of $\mu\mu\ell$ and $e\mu\ell$ from [5] and a newly updated $\mu^\pm\mu^\pm$ analysis [8] using the modified frequentist approach. The fraction of signal events that is selected by more than one selection is assigned to the selection with the largest signal-to-backround ratio and removed from all others. The expected and observed limits are shown in figure 5 as a function of $\tilde{\chi}_1^\pm$mass. This result improves significantly the upper limit of about 0.2 pb set by [5]. The cross section limit set in this analysis corresponds to a chargino mass limit of 140 GeV in the 3ℓ-max scenario.

TABLE IV: Number of signal events expected at different stages of the selection. For the final cut, also the signal efficiency is presented. Efficiencies are normalized to lepton events with all flavour combinations.

Cut	LHA.244.324	LHA.131.232	LHA.87.194
(1) Presel	8.24±0.04	18.0±0.10	26.8±0.14
(2) Anti-Z	5.18±0.03	13.0±0.07	20.5±0.10
(3) Isolated track	2.96±0.02	7.60±0.03	10.4±0.06
(4) $\not\!\!E_T$ related	2.20±0.01	4.64±0.02	6.39±0.03
(5) Tr×$\not\!\!E_T$	1.69±0.01	3.45±0.01	4.73±0.02
efficiency (3ℓ) [%]	3.16	2.64	2.41

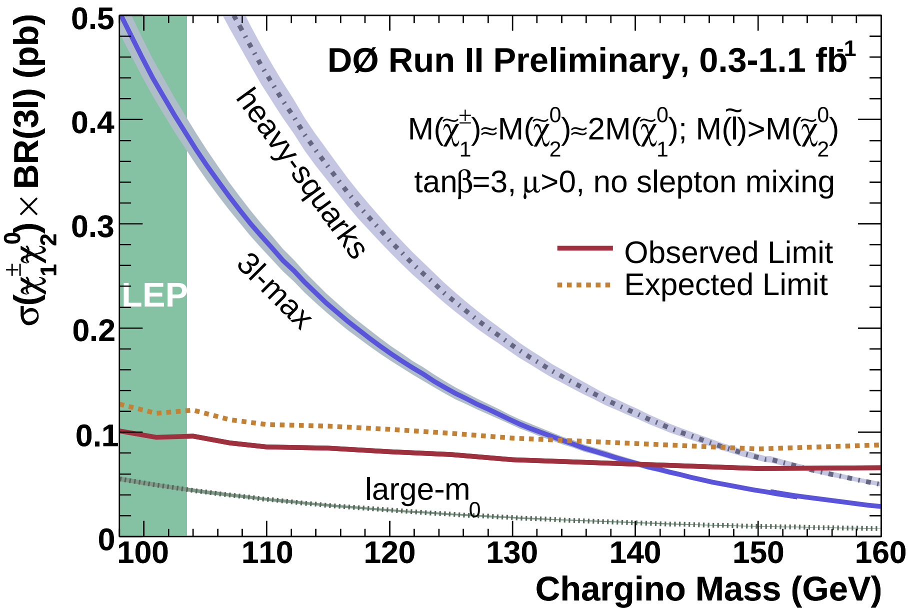

FIG. 5: Limit on $\sigma \times \mathrm{BR}(3\ell)$ as a function of $\tilde{\chi}_1^\pm$ mass, in comparison with the expectation for several SUSY scenarios. The red line corresponds to observed mSUGRA limit. PDF and renormalization/factorization scale uncertainties are shown as shaded bands.

VI. CONCLUSIONS

A search has been performed for the trilepton decay signature from the associated production of the lightest chargino and the next-to-lightest neutralino in leptonic channels with two electrons, using data corresponding to an integrated luminosity of 1.1 fb^{-1}. No evidence for supersymmetry is observed and upper limits on the product of cross section and leptonic branching fraction are set, which improve previous limits set. Chargino mass limits beyond the reach of LEP chargino searches are derived for several SUSY reference scenarios with enhanced leptonic branching fractions.

Acknowledgments

We thank the staffs at Fermilab and collaborating institutions, and acknowledge support from the Department of Energy and National Science Foundation (USA), Commissariat à l'Energie Atomique and CNRS/Institut National de Physique Nucléaire et de Physique des Particules (France), Ministry of Education and Science, Agency for Atomic Energy and RF President Grants Program (Russia), CAPES, CNPq, FAPERJ, FAPESP and FUNDUNESP (Brazil), Departments of Atomic Energy and Science and Technology (India), Colciencias (Colombia), CONACyT (Mexico), KRF (Korea), CONICET and UBACyT (Argentina), The Foundation for Fundamental Research on Matter (The Netherlands), PPARC (United Kingdom), Ministry of Education (Czech Republic), Natural Sciences and Engineering Research Council and WestGrid Project (Canada), BMBF (Germany), A.P. Sloan Foundation, Civilian Research and Development Foundation, Research Corporation, Texas Advanced Research Program, and the Alexander von

Humboldt Foundation.

[1] H.P. Nilles, Phys. Rep. **110** (1984) 1;
H.E. Haber and G.L. Kane, Phys. Rep. **117** (1985) 75.
[2] W.Beenakker *et al.,* '*The production of Charginos/Neutralinos and Sleptons at Hadron Colliders* ", hep-ph/9906298.
[3] LEPSUSYWG, ALEPH, DELPHI, L3 and OPAL experiments,
note LEPSUSYWG/01-07.1, (`http://lepsusy.web.cern.ch/lepsusy /Welcome.html`)
[4] B.Abbott *et al.,* Phys. Rev. Lett. **80** (1998) 8.
[5] V. Abazov*et al.,* (DØ Collaboration), '*Search for supersymmetry via associated production of charginos and neutralinos in final states with three leptons* ", Phys. Rev. Lett. **95** (2005) 8.
[6] F. Abe *et al.,*(DØ Collaboration) '*Search for Chargino-Neutralino Associated Production at the Fermilab Tevatron Collider* ", Phys. Rev. Lett. **80**, 5275 (1998).
[7] T. Sjostrand, Comp. Phys. Commun. **82** (1994) 74, `CERN-TH 7112/93` (1993).
[8] V. Lesne, '*Search for the associated production of charginos and neutralinos in like sign dimuon channel* DØ note 5126
[9] P. Skands *et al.,* JHEP 07, 036 (2004),
[10] J. Kozminski, R. Kehoe, H. Weerts, S. Park, A. Quadt, J. Gardner, Sh. Jabeen, *"Electron Likelihood in p14"*, DØ Note 4449.